

Room-temperature synthesized carbon quantum dots and potential applications to cell imaging

Q. Huang^a, Z. Y. Zhou^b, Q. Lv^{a,*}

^a*Clinical Medicine Research Center, Xinqiao Hospital, Army Medical University (Third Military Medical University), Chongqing 400038, China*

^b*92914 Army Hospital, People's Liberation Army of China, Hainan 571800, China*

Carbon quantum dots (CQDs) with excellent properties have attracted attention owing to wide applications in many fields. In this paper, we report a method to synthesize CQDs at room temperature without any external energy supply and energy-catalyzing reagents. The characterization results indicate that the CQDs have good dispersion and water solubility, the averaged dimension is around 5.37 nm, consisting mainly of C, O, N, and S elements, the fluorescence quantum yield was 8.72%. In addition, the experimental results show that CQDs have excellent optical stability and good biocompatibility, which can be used in the field of cellular imaging.

(Received; November 27, 2022; Accepted February 8, 2023)

Keywords: Carbon quantum dots, Room temperature synthesis, Glutathione, High biocompatibility, Fluorescent probes, Cell imaging

1. Introduction

Carbon quantum dots (CQDs) are an emerging eco-friendly carbon nanomaterial with excellent performance (size <10 nm), with sp^2 hybrid structure and rich surface functional groups like amino (-NH₂), hydroxyl (-OH), and carboxyl (-COOH)^[1]. Due to the excellent photostability, high specific surface area and fluorescence quantum yield, good electron mobility, and low-cost source of CQDs^[2, 3], making they are widely used in various fields such as photoelectric conversion^[4, 5], molecular detection^[6], nano-drug delivery^[7-9], and catalysis^[10] in the past decade. In addition, the biocompatibility and safety of carbon quantum dots are beneficial for their application in bioimaging. Conventional metal quantum dots are often used as bioimaging agents, but their high toxicity hinders their application in living tissues, while carbon quantum dots can well overcome this shortcoming^[11, 12]. Some researchers have discovered that the fluorescence of carbon quantum dots comes from the quantum confinement of conjugated π -electrons in the sp^2 carbon-network and can be accurately regulated with its dimensions, edge conformation, shape, surface functional groups, and heteroatom doping^[13].

CQDs are usually prepared in two ways: "bottom-up" or "top-down". The "bottom-up" approach uses precursors (e.g., polymers, carbon-containing compounds, or organic acids) to prepare CQDs by strong acid carbonization, microwave-assisted, solvent thermal, or hydrothermal

* Corresponding author: 15023181652@163.com
<https://doi.org/10.15251/DJNB.2023.181.195>

treatments^[14]. In contrast, the "top-down" approach uses carbon materials such as carbon nanotubes or graphite to prepare CQDs by laser ablation, electrochemical oxidation, chemical oxidation, ultrasonic treatment, etc.^[15]. These synthesis methods usually require more complex steps, bulky experimental apparatus, or higher preparation temperatures. This not only generates large energy consumption and increases the cost, but also may use environmentally unfriendly strong acid reagents, which greatly limit them to large-scale manufacturing and deeper commercial applications. Thereby, it is relevant to explore simpler, energy-saving, green, and scalable room temperature synthesis methods.

In this paper, biocompatible carbon quantum dots (CQDs) were produced by a one-step approach using glutathione as a precursor at room temperature (Figure 1). To our knowledge, this is the first presentation of room-temperature preparation of fluorescent CQDs without any external energy supply and energetic catalytic reagents. The results of transmission electron microscopy (TEM), Fourier transform infrared spectra (FTIR), X-ray photoelectron spectra (XPS), and fluorescence spectra (FL) characterization showed that CQDs with a maximum excitation wavelength of 363 nm and emission wavelengths of 442 nm. The quantum yield of CQDs was 8.72%, which is a potential bioimaging agent. The CQDs have good dispersibility and water solubility, with a dimension is around 5.37 nm, and are mainly consisted of C, O, N, and S elements with rich surface functional groups including C=O, -OH, C=C, and C-N. In addition, the experimental results show that CQDs have excellent optical stability as well as good biocompatibility for cell imaging applications.

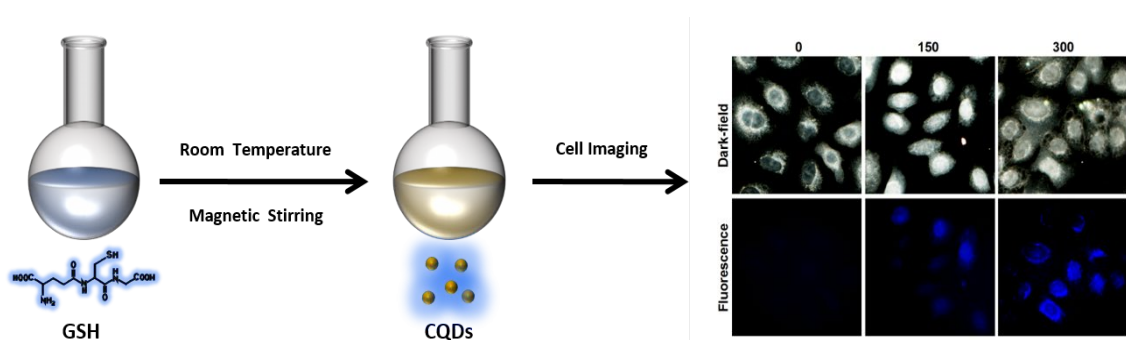


Fig. 1. Room temperature synthesis and cell imaging of CQDs.

2. Materials and methods

2.1. Main instruments and reagents

Tecnai G2 F20 S-TWIN high-resolution transmission electron microscope (FEI, USA); Thermo escalab 250Xi photoelectron spectrometer (ThermoFisher Scientific, UK); Iraffinity-1 Fourier transform infrared spectrometer (Shimadzu, Japan). Persee TU-1901 UV-Vis spectrophotometer (Beijing Puginye General Instrument Co., Ltd., China); PerkinElmer LS-55 fluorescence spectrometer (Perkin-Elmer, USA); BX63 fluorescence microscope (Olympus, Japan).

Reduced glutathione (GSH) (Shanghai Bioengineering Co., Ltd.); sodium carbonate, sodium bicarbonate (Chengdu Kelong Chemical Reagent Farm); dialysis bag (Viskase, USA);

quinine sulfate, fluorescein (Xiangzhong Geological Experimental Research Institute, China); A549 lung adenocarcinoma cell line (ATCC, USA); 1640 cell culture medium (Gibco, USA); fetal bovine serum (FBS) (Hangzhou Four Seasons Green); 0.25% trypsin solution (HyClone, USA); penicillin-streptomycin solution (Shanghai Biyuntian); the reagents used during the experiment were not treated before use, and ultrapure water was homemade from the laboratory.

2.2. Preparation of CQDs

0.5 g of GSH was dissolved in 100 mL of $\text{NaHCO}_3\text{-Na}_2\text{CO}_3$ buffer solution (pH=6.88), and the mixture was stirred slowly at room temperature for several days, and the colorless transparent solution gradually changed to the yellow transparent solution. Subsequently, the obtained yellow transparent solution was purified by dialysis bag (MW: 500 Da) to remove the unreacted compounds.

2.3. Biocompatibility of CQDs

Lung cancer human alveolar basal epithelial cells (A549) were cultured with 1640 complete medium (supplemented with 10 % FBS, 0.1 mg/mL streptomycin, and 100 U/mL penicillin) in an incubator at 37 °C, saturated humidity, and 5 % CO_2 .

The toxicity of CQDs to cells was determined using the CCK-8 method. A549 cells were inoculated into 96-well plates at 1×10^5 cells per well and cultured at 5% CO_2 , 37 °C for 12 h. The original medium was removed and replaced with medium including various concentrations of CQDs (0, 25, 50, 100, 150, 200, 250, 300, 400, and 500 $\mu\text{g/mL}$) and continued to incubate for 24 h. 10 μL of CCK-8 was added to each well and incubated for 2 h. Cell viability was evaluated using absorbance at 450 nm. Cell survival rate = $[(A_{\text{sample}} - A_{\text{blank}})/(A_{\text{control}} - A_{\text{blank}})] \times 100\%$.

A_{sample} is the absorbance of the sample wells (CCK-8 solution with cells and CQDs); A_{control} is the absorbance of the control wells (CCK-8 solution with cells, without CQDs); and A_{blank} is the absorbance of the blank wells (CCK-8 solution without cells or CQDs)

2.4. Cell imaging

A549 cells were inoculated into 6-well plates with 1×10^6 cells per well and cultured at 5% CO_2 and 37 °C for 12 h. The original medium was removed and replaced with a medium including various concentrations of CQDs (0, 150, 300 $\mu\text{g/mL}$) for 24 h. The cells were rinsed three times using phosphate buffered solution (PBS) to remove excess CQDs. The cells were fixed with 2 mL of anhydrous methanol for 10 min, the fixative was aspirated and discarded, and then the cells were rinsed three times using PBS and observed with fluorescence microscopy for photographs.

3. Results and discussion

3.1. Synthesis and characterization of CQDs

CQDs were obtained through dissolving 0.5 g GSH in 100 mL $\text{NaHCO}_3\text{-Na}_2\text{CO}_3$ buffer solution and stirring slowly at room temperature for 11 days. The morphological characteristics of CQDs were investigated with transmission electron microscopy (TEM). As illustrated in Figure 2a, CQDs were monodisperse sphere-like nanoparticles with a dimension is around $5.37 \text{ nm} \pm 0.91 \text{ nm}$ (Figure 2b). High-resolution TEM showed that the lattice spacing of CQDs was 0.329 nm

(Figure 2c). X-ray energy spectroscopy (EDX) indicated that CQDs were mainly composed of C, O, N, and S (Figure 2d).

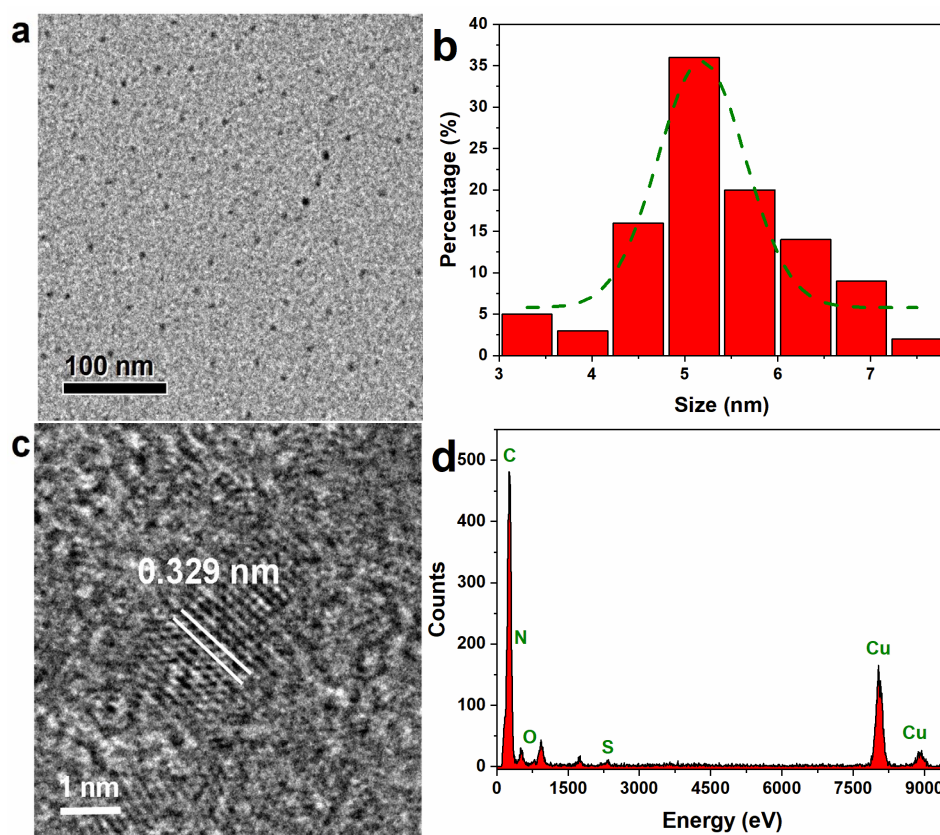


Fig. 2. Morphological characterization of CQDs: (a) TEM photos of CQDs. (b) Dimensional distribution map of CQDs. (c) High-resolution TEM photos of CQDs with a lattice spacing of 0.329 nm. (d) EDX spectrum of CQDs.

The CQDs were further characterized using X-ray photoelectron spectra (XPS). The results show that CQDs are mainly consisted of C, O, N, and S (Figure 3a), which is consistent with the EDX results. The four characteristic peaks at 284.98 eV, 531.13 eV, 399.72 eV, and 167.71 eV correspond to C1s, O1s, N1s, and S2p, with elemental content percentages of 52.46%, 32.57%, 10.34%, and 4.63%, respectively. High-resolution XPS spectra of C1s of CQDs showed the presence of three forms of C elements: 284.84 eV (C=C/C-C), 285.85 eV (C-O), and 287.91 eV (C=O/C=N) (Figure 3a, inset)^[16-18]. Figure 3b shows the Fourier infrared spectra (FTIR) of CQDs and GSH. The 1714 cm^{-1} and 1404 cm^{-1} belong to the characteristic peaks of C-OH and -COOH, respectively. The broad peak around 3443 cm^{-1} should be owed to the characteristic stretching vibrations of hydroxyl and amino groups, and the absorption peak at 1633 cm^{-1} is a C=C stretching vibration peak. A typical S-H stretching vibration peak (2525 cm^{-1}) was investigated in the FTIR spectra of GSH, which disappeared after the formation of CQDs. The mentioned results indicate that GSH successfully formed CQDs and that functional groups such as amino, hydroxyl, carboxyl, and C=C are present on the surface^[19].

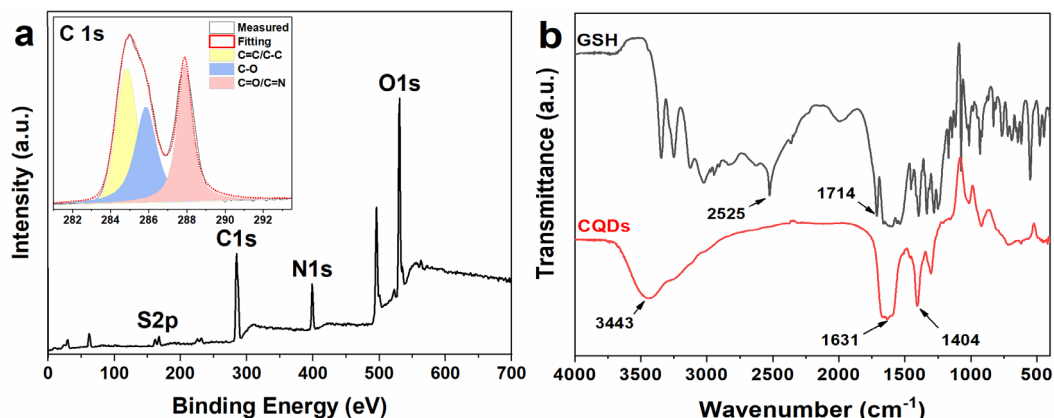


Fig. 3. Characterization of the structural composition of CQDs: (a) XPS spectra of CQDs. Inset: high-resolution XPS C1s spectrum. (b) FTIR spectra of GSH and CQDs.

3.2. Optical characterization of CQDs

The UV-Vis absorption spectra and fluorescence spectrum reveal the optical characterization of CQDs (Figure 4). The CQDs have absorption peaks at 228 nm, which may be attributed to the $\pi \rightarrow \pi^*$ leap of the aromatic ring^[20, 21]. In addition, the UV-Vis absorption spectrum of CQDs is distinctly different from GSH, CQDs have a broad absorption peak after 238 nm and the tail extends into the visible range, which may be attributed to the $n \rightarrow \pi^*$ leap of doped heteroatoms (e.g., S and N)^[22]. It is well known that fluorescence is one of the most distinctive features of CQDs, and fluorescence spectra show that CQDs have a maximum emission wavelength of 442 nm and a maximum excitation wavelength of 363 nm. Bright blue fluorescence was observed with 365 nm UV light irradiation (Figure 4, inset). With quinine sulfate as a referent, the relative luminescence quantum yield (QY) of CQDs was 8.72%, which exhibited a high fluorescence efficiency.

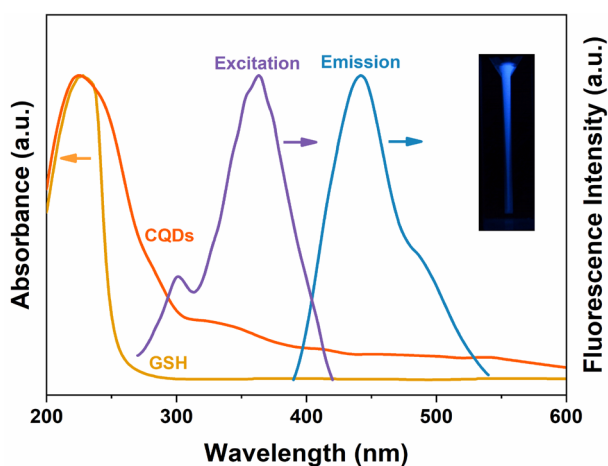


Fig. 4. Optical characterization of CQDs: UV-Vis absorption spectra, fluorescence excitation spectra, and emission spectra of CQDs (363 nm excitation). Inset: fluorescence image of CQDs under 365 nm light irradiation.

The formation of CQDs was probed using fluorescence signals, and the fluorescence intensity stabilized from the rising state when GSH was dissolved in $\text{NaHCO}_3\text{-Na}_2\text{CO}_3$ buffer solution with stirring at room temperature for 11 days (Figure 5a), indicating the formation of structurally stable CQDs, and the successful synthesis of fluorescent CQDs at room temperature without any external energy supply and energy-catalyzing reagents. Moreover, compared with fluorescein, the fluorescence of CQDs decreased less under continuous irradiation with 365 nm UV light, showing better resistance to photostability (Figure 5b). The mentioned results indicate that CQDs have good optical stability, which is beneficial for their wide application in biomedical fields. which is beneficial for a wide range of applications in biomedicine.

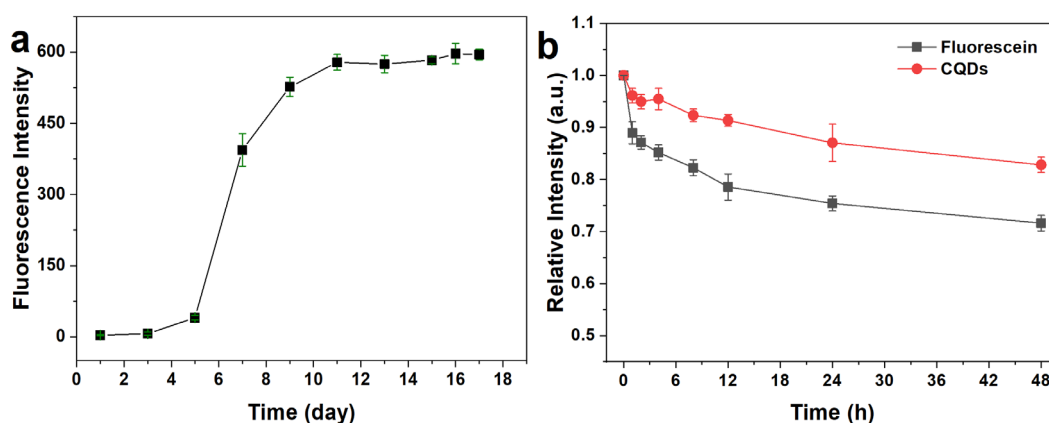


Fig. 5. (a) The change in fluorescence intensity of CQDs depends on reaction time. (b) The relative fluorescence intensity (I/I_0) of fluorescein and CQDs with time under continuous UV light irradiation.

3.3. Cellular imaging with CQDs

Biocompatibility is a prerequisite for the application of CQDs in bioimaging. The in vitro cytotoxicity of CQDs on A549 cells was detected by the CCK-8 assay. As demonstrated in Figure 6a, the CQDs had no significant effect on the viability of A549 cells when cells were incubated by various concentrations of CQDs (25-500 $\mu\text{g/mL}$) for 24 h. The cell survival rate remained above 80% even at CQDs concentrations up to 500 $\mu\text{g/mL}$. This indicates that CQDs have good biocompatibility and have the potential as bioimaging probes. As shown in Figure 6b, the A549 cells after incubation with different concentrations of CQDs showed concentration-dependent blue fluorescence, while no fluorescence was observed in the control cells. This indicates that CQDs can be taken up by cells to enter the cell interior and can be applied in the field of cellular fluorescence imaging.

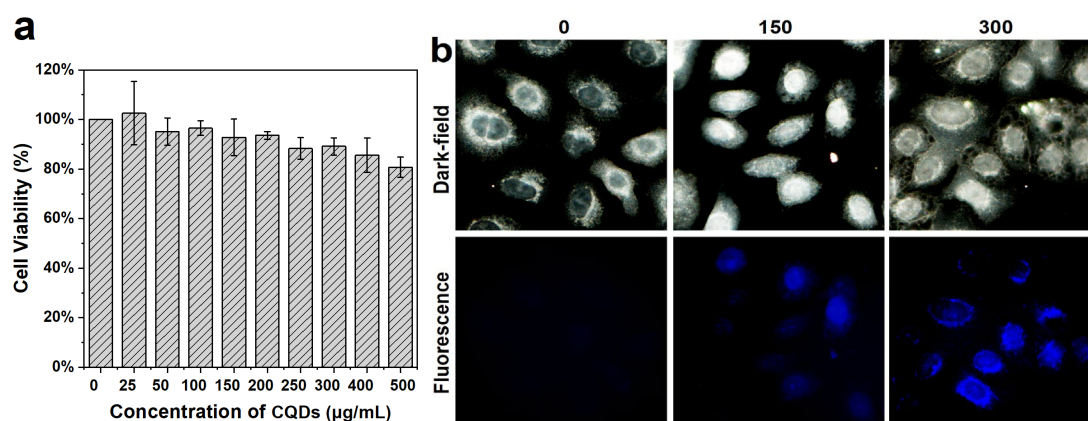


Fig. 6. Imaging applications of CQDs: (a) Survival rate of A549 cells after incubation by various concentrations of CQDs for 24 h, $n=3$. (b) Dark-field light scattering and fluorescence images of A549 cells after incubation with CQDs ($\mu\text{g/mL}$).

4. Conclusion

In summary, we report a method for the preparation of fluorescent CQDs at room temperature without any external energy supply and energy-catalyzed reagents. Compared with previously reported methods for the preparation of carbon quantum dots, the CQDs synthesis strategy in this paper is more facile, energy-saving, and environmentally friendly. The prepared CQDs exhibit good dispersion and water solubility with a dimension is around 5.37 nm, and are mainly consisted of C, O, N, and S elements with rich surface functional groups like -OH, C=O, C-N, and C=C. Its maximum excitation and emission wavelengths are 363 nm and 442 nm, respectively, and its quantum yield is 8.72%. Its excellent optical stability makes it successfully applied in the field of cell imaging. This research not only opens up a new efficient pathway for the greener preparation of fluorescent CQDs, but also reveals their promising applications in optical sensing and biomedicine.

Acknowledgements

This work was supported by the platform of the Clinical Medical Research Center of the Second Affiliated Hospital (Xinqiao Hospital) of the Army Medical University

References

- [1] Du J, Xu N, Fan J, et al., *Small*, 2019,15(32):e1805087; <https://doi.org/10.1002/sml.201805087>
- [2] Yu Long Y, Xin Sheng, *Analyst*, 2016,141(9):2619-2628; <https://doi.org/10.1039/C5AN02321A>

- [3] Jaleel J A, Pramod K., *Journal of Controlled Release*, 2018,269:302-321;
<https://doi.org/10.1016/j.jconrel.2017.11.027>
- [4] Guo C X, Yang H B, Sheng Z M, et al., *Angewandte Chemie International Edition*, 2010,49(17):3014-3017; <https://doi.org/10.1002/anie.200906291>
- [5] Guo X, Wang C, Yu Z, et al., *Chemical Communications*, 2012,48(21):2692-2694;
<https://doi.org/10.1039/c2cc17769b>
- [6] Zhu S, Meng Q, Wang L, et al., *Angewandte Chemie International Edition*, 2013,52(14):3953-3957; <https://doi.org/10.1002/anie.201300519>
- [7] Wang Y, Chen L., *Nanomedicine: Nanotechnology, Biology and Medicine*, 2011,7(4):385-402;
<https://doi.org/10.1016/j.nano.2010.12.006>
- [8] Huang P, Lin J, Wang X, et al., *Advanced Materials*, 2012,24(37):5104-5110;
<https://doi.org/10.1002/adma.201200650>
- [9] Hola K, Zhang Y, Wang Y, et al., *Nano Today*, 2014,9(5):590-603;
<https://doi.org/10.1016/j.nantod.2014.09.004>
- [10] Liu J, Liu Y, Liu N, et al., *Science*, 2015,347(6225):970;
<https://doi.org/10.1126/science.aaa3145>
- [11] Liu C, Zhang P, Zhai X, et al., *Biomaterials*, 2012,33(13):3604-3613;
<https://doi.org/10.1016/j.biomaterials.2012.01.052>
- [12] Chatzimitakos T, Kasouni A, Sygellou L, et al., *Talanta*, 2017,175:305-312;
<https://doi.org/10.1016/j.talanta.2017.07.053>
- [13] Miao X, Qu D, Yang D, et al., *Advanced Materials*, 2018,30(1);
<https://doi.org/10.1002/adma.201704740>
- [14] Cohen E N, Kondiah P, Choonara Y E, et al., *Current Pharmaceutical Design*, 2020,26(19):2207-2221; <https://doi.org/10.2174/1381612826666200402102308>
- [15] Wang R, Lu K, Tang Z, et al., *Journal of Materials Chemistry A*, 2017,5(8):3717-3734;
<https://doi.org/10.1039/C6TA08660H>
- [16] Cheng C, Shi Y, Li M, et al., *Materials for Biological Applications*, 2017,79:473-480;
<https://doi.org/10.1016/j.msec.2017.05.094>
- [17] Wang X, Zhang Y, Zhang M, et al., *Molecules*, 2019,24(22);
<https://doi.org/10.3390/molecules24224152>
- [18] Kong H, Zhao Y, Zhu Y, et al., *Artif Cells Nanomed Biotechnol*, 2021,49(1):11-19;
<https://doi.org/10.1080/21691401.2020.1862134>
- [19] Yang L, Wang D, Gong Y, et al., *Spectrochim Acta A Mol Biomol Spectrosc*, 2022,286:121963; <https://doi.org/10.1016/j.saa.2022.121963>
- [20] Jin J C, Yu Y, Yan R, et al. N, *ACS Applied Bio Materials*, 2021,4(6):4973-4981;
<https://doi.org/10.1021/acsbm.1c00242>
- [21] Cardoso M A, Duarte A J, Gonçalves H., *Analytica Chimica Acta*, 2022,1202:339654;
<https://doi.org/10.1016/j.aca.2022.339654>
- [22] Xu Y, Jia X H, Yin X B, et al., *Analytical Chemistry*, 2014,86(24):12122-12129;
<https://doi.org/10.1021/ac503002c>